IOP Publishing Physica Scripta
Phys. Scr. 95 (2020) 065802 (8pp) https://doi.org/10.1088/1402-4896/ab7c76

Multiphase coexistence and enhanced piezoelectric properties in $(1-x)(K_{0.45}Na_{0.55})(Nb_{0.965}Sb_{0.035})O_3$ _ $xBi_{0.5}(K_{0.91}Li_{0.09})_{0.5}(Hf_{0.3}Zr_{0.7})O_3$ lead-free ceramics

Yongqi Pan, Xiaowei Dai, Jingchuan Li, Yunhe Yi, Yungang Yu, Caiwang He, Yunyi Liu, Yunjie Xiang and Yi Chen[1]

School of Materials and Energy, Southwest University, Chongqing 400715, People's Republic of China

E-mail: mrchenyi@swu.edu.cn

Received 18 September 2019, revised 1 January 2020
Accepted for publication 4 March 2020
Published 20 March 2020

Abstract

A new lead-free piezoelectric solid solution system with the formula of $(1-x)(K_{0.45}Na_{0.55})(Nb_{0.965}Sb_{0.035})O_3$_$xBi_{0.5}(K_{0.91}Li_{0.09})_{0.5}(Hf_{0.3}Zr_{0.7})O_3$ were prepared using a conventional solid-phase sintering method, and we investigated the relationship between the composition, microstructure, phase structure and electrical properties of the ceramics. It was found that adding $Bi_{0.5}(K_{0.91}Li_{0.09})_{0.5}(Hf_{0.3}Zr_{0.7})O_3$ induced the ceramics transition from a single orthorhombic structure to a coexistence of multiple phases, and a three-phase coexistence of rhombohedral, orthorhombic and tetragonal phases was present in the composition range $x = 0.03$ to 0.035. Enhanced piezoelectric properties were obtained for the ceramics near the three-phase coexistence region, with the largest piezoelectric constant d_{33} of 253 pC/N and the highest planar electromechanical coupling coefficient of 0.36. Additionally, a rough phase diagram for the solid solution system was established by using the critical temperatures determined by the temperature-dependent dielectric properties. The authors believe that these results can provide a useful reference for the development of $(K,Na)NbO_3$-based lead-free piezoelectric ceramics.

Keywords: lead-free ceramics, piezoelectric properties, multiphase coexistence, perovskites, dielectric properties

(Some figures may appear in colour only in the online journal)

1. Introduction

Traditional lead-based piezoelectric ceramics, represented by $Pb(Zr,Ti)O_3$ (PZT)-based ceramics, have been used in many electronic devices, such as actuators, resonators and transducers [1, 2]. Unfortunately, lead-based piezoelectric ceramics can cause a huge damage to both the environment and human health, because of the toxic lead oxide constituting over 60 wt% of their raw materials [3–5]. Therefore, developing lead-free piezoelectric materials with high performances has been an urgent duty. The $(K,Na)NbO_3$ (KNN)-based ceramics are widely considered to be among the most promising lead-free piezoelectric materials for the replacement of lead-based ones, due to their excellent piezoelectric properties and relatively high Curie temperature (T_C) [6–10]. However, although some KNN-based ceramics have exhibited piezoelectric properties comparable to that of some commercial PZT-based ones [11–13], there still exist some

[1] Author to whom any correspondence should be addressed.

issues that hinder their practical use, such as a very narrow sintering interval and an extremely strong composition dependence of piezoelectric activity [10, 14].

Over the past many years, a large number of researchers have committed to improving the piezoelectric performances of KNN-based ceramics by the way of chemical modifications and/or using new preparation methods [3–20]. For example, Saito *et al* [20] in 2004 reported a giant piezoelectric constant ($d_{33} = 416$ pC/N) obtained in the Li^+, Ta^{5+} and Sb^{5+} modified KNN-based ceramics fabricated by the reactive templated grain growth technique (RTGG). However, the high cost of RTGG is a main limitation for its widespread use. By contrast, the chemical modification is a more economical method and thus is more likely suitable for large-scale commercial production. Especially, the chemical modification can readily result in the formation of a phase boundary (i.e., a coexistence of multiple phases), which may usually bring about an enhanced piezoelectric activity [15–19].

There are three types of phase boundaries in KNN-based ceramics, including rhombohedral-orthorhombic (R–O), orthorhombic-tetragonal (O–T) and rhombohedral-tetragonal (R–T) phase boundaries [21–23]. The ceramics with an R–T phase boundary generally possess higher piezoelectric properties than that of the ceramics with an R–O or an O–T phase boundary, and therefore have been a research hotspot [11–13, 21–23]. It is through modifying the temperature of R–O phase transition (T_{R-O}) and/or the temperature of O–T phase transition (T_{O-T}) to room temperature that a phase boundary is constructed in KNN-based ceramics [21–23]. Many additives can modify the T_{R-O} or T_{O-T} to room temperature after adding appropriate amount of them into KNN, including ion substitutions such as Li^+, Sb^{5+} and Ta^{5+} ions [24–26], as well as ABO_3-type compounds such as $BaZrO_3$ and $BiScO_3$ [27, 28]. Particularly, some additives [e.g., $Bi_{0.5}Na_{0.5}ZrO_3$ (BNZ)] [29] can make the T_{R-O} and T_{O-T} simultaneously move towards room temperature and thereby have attracted wide attention, as they are able to provide a great help for the construction of R-T phase boundary. It is worth mentioning that the R-T phase boundary identified in many references is actually a three-phase coexistence region of rhombohedral, orthorhombic and tetragonal phases (R–O–T) [30, 31], so it is perhaps more accurate to call it R–O–T phase boundary.

In this study, we designed the $(1-x)(K_{0.45}Na_{0.55})(Nb_{0.965}Sb_{0.035})O_3-xBi_{0.5}(K_{0.91}Li_{0.09})_{0.5}(Hf_{0.3}Zr_{0.7})O_3$ [abbreviated as $(1-x)$KNNS-xBKLHZ] system piezoelectric ceramics through adding Sb^{5+} ions and ABO_3-type compound BKLHZ into KNN. The added Sb^{5+} can increase the T_{R-O} [32], while the Li^+ contained in BKLHZ is able to reduce the T_{O-T} [24]. As for BKLHZ, it should have similar effects on the two temperatures as BNZ, because elements contained in both of them respectively belong to the three same groups of periodic table. Therefore, an R–O–T phase boundary predictably can be built up in the new solid solution system via adding suitable amount of it. An investigation was performed on the relationship between composition, phase structure and electrical properties of the $(1-x)$KNNS-xBKLHZ ceramics, and enhance piezoelectric properties were found to be achieved for the ceramics with compositions near the R–O–T phase boundary.

2. Experimental details

Lead-free $(1-x)$KNNS-xBKLHZ piezoelectric ceramics were prepared by a conventional ceramic synthetic route. High purity carbonates and oxides powder including K_2CO_3 (99.0%), Na_2CO_3 (99.8%), Nb_2O_5 (99.5%), Sb_2O_3 (99.5%), Bi_2O_3 (99.0%), Li_2CO_3 (98.0%), HfO_2 (99.99%) and ZrO_2 (99.0%) were used as raw materials. After accurately weighing, the raw materials powders were ball-milled in absolute ethanol for 24 h. The slurry was dried and then calcined at 850 °C for 6 h. After grinding again, the calcined powders were granulated into granules using 3–5 wt% polyvinyl alcohol (PVA) as an adhesive. Afterwards, the granules were pressed into disc pellets with a diameter of ~10 mm and a thickness of ~1 mm in a die using a unidirectional pressure of 10 MPa. Following the burnout of the PVA at 500 °C for 2 h, the pellets were air-sintered at 1100–1150 °C (determined on the composition) for 3 h and then cooled to room temperature in the furnace. For the measurement of electrical properties, both the surfaces of the pellets were coated with a silver paste and subsequently were fired at 600 °C for 10 min to form electrodes.

An x-ray diffractometer (XRD-7000, Shimadzu, Japan) was employed to identify the phase structures of the $(1-x)$ KNNS-xBKLHZ ceramic samples using Cu $K\alpha_1$ irradiation ($\lambda = 0.154056$ nm), and their surface morphologies were observed by a scanning electron microscopy (SEM). The temperature-dependent dielectric properties were measured in the temperature range from around −100 °C to 150 °C as well as from room temperature to 450 °C by using a computer-controlled LCR analyzer (E4980A, Keysight Technologies, USA) together with a specially designed multi-sample furnace. For the measurement of piezoelectric properties, the silver-coated ceramic samples were immersed in a room-temperature silicone oil bath, applying a dc electric field of 4 kV/mm on the two surfaces of the ceramic pellets for 30 min. After aging the poled ceramic samples for 24 h, their piezoelectric constant d_{33} and planar electromechanical coupling coefficient (k_p) were determined with a quasi-static d_{33} meter (YE2730A, Wuxi Yutian, China) and a resonance-antiresonance method using an impedance analyzer (ZX70A, Changzhou Zhixin, China), respectively.

3. Results and discussion

Figure 1 shows the SEM surface microstructures of the $(1-x)$ KNNS-xBKLHZ ceramics. It can be found that all the grains are in a cuboidal shape, implying that no liquid phase appeared during the sintering step. Additionally, one can note that all the compositions exhibit an obviously bimodal distribution in grain sizes that both large and small grains exist simultaneously, and this is a phenomenon frequently occurred in KNN-based ceramics with Sb^{5+} or Zr^{4+} ions [33]. This

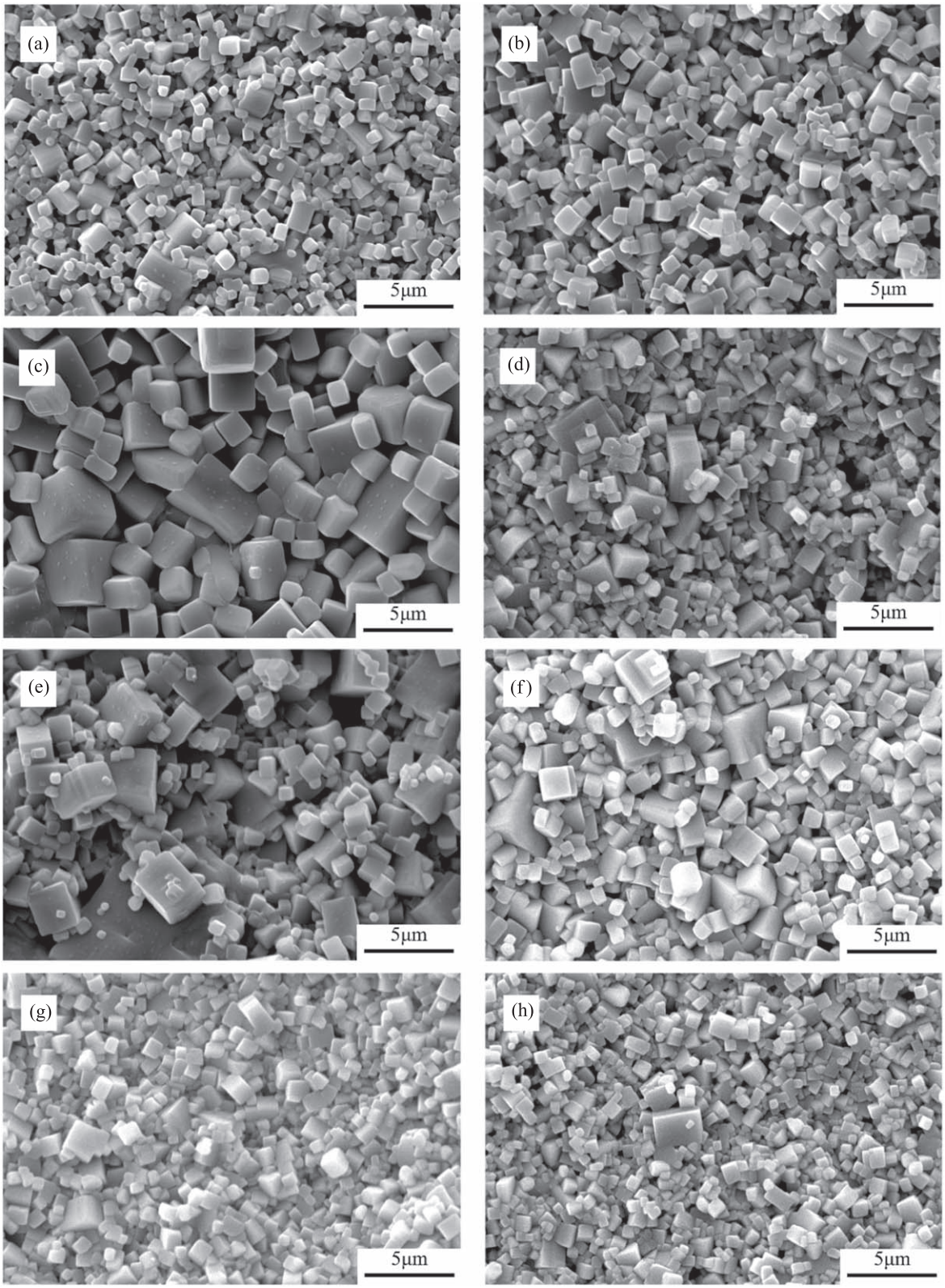

Figure 1. SEM surface micrographs of the $(1-x)$KNNS-xBKLHZ ceramics with (a) $x = 0$; (b) $x = 0.01$; (c) $x = 0.02$; (d) $x = 0.025$; (e) $x = 0.03$; (f) $x = 0.035$; (g) $x = 0.04$; (h) $x = 0.05$.

phenomenon is usually considered to be caused by the accumulation of these added ions at the grain boundaries [33]. Furthermore, a few pores can be seen in the microstructures of all compositions, which may lead to a low breakdown voltage and thus is adverse to the polarization of the ceramics. The pores are difficult to eliminate for the KNN-based ceramics prepared by a traditional solid-state preparation method, especially for the ones containing Sb^{5+} ions [25]. Many new

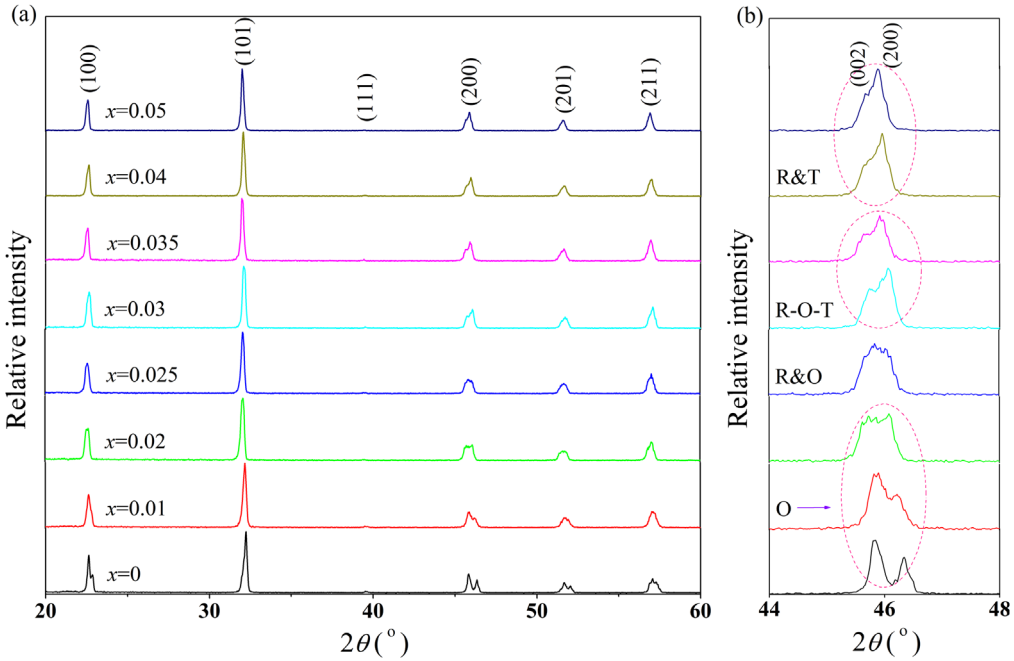

Figure 2. Room-temperature XRD patterns of the (1-*x*)KNNS-*x*BKLHZ ceramics in the 2θ range of (a) 20–60° and (b) 44–48°.

ceramic preparation methods, such as citrate sol-gel method [34], have been found to result in a highly dense microstructure with few flaws, therefore may be tried to be used in the fabrication of KNN-based ceramics in future researches.

Figure 2(a) depicts the room-temperature XRD patterns of the (1−*x*)KNNS-*x*BKLHZ ceramics, measured in the 2θ range of 20–60°. All the ceramics should have a pure perovskite structure because none of the XRD peaks in the patterns can be identified as belonging to any other phases, which suggests that the added BKLHZ has diffused into the lattice of KNNS completely. For better observation on the structural evolution of the ceramics, the enlarged views of their XRD patterns between $2\theta = 44°$ and 48° are exhibited in figure 2(b). One can notice an obvious decrease in the relative intensity of (002) and (200) peaks (I_{002}/I_{200}) with the increase of *x*, implying that there is a structural variation in the studied composition range.

Dielectric-temperature measurements from about −100 to 150 °C were carried out to further determine the phase structures of the (1-*x*)KNNS-*x*BKLHZ ceramics, as illustrated in figure 3. There are two dielectric anomalies existing on the curves for the compositions $x = 0$ to 0.035, which respectively correspond to the T_{R-O} and T_{O-T}, as indicated in the figure. The ceramics with compositions $x = 0$ to 0.02 should possess a single orthorhombic structure as the two temperatures of them both are far from room temperature, while the composition $x = 0.025$ has a two-phase coexistence of R-O phases, because its T_{R-O} is at around room temperature. For compositions $x = 0.03$ to 0.035, both the T_{R-O} and T_{O-T} are near the room temperature, so they can be identified as possessing a coexistence of three phase including rhombohedral, orthorhombic and tetragonal phases, as suggested by [30, 31]. The T_{R-O} and T_{O-T} merge into each other at $x = 0.04$, which is an indication of the formation of R–T phase coexistence. The temperatures of the R–T phase coexistence (T_{R-T}) are all a little above room temperature for the ceramics with compositions $x = 0.04$ to 0.05, so they have the possibility of possessing a pure rhombohedral structure at room temperature. But this is negated by the fact that the shape of their XRD peaks at about 45° is obviously asymmetric as observed in figure 2(b), indicating that they are not a real single peak like that of pure rhombohedral KNN-based ceramics [17–19]. Therefore, they should have a two-phase coexistence of R–T phases at room temperature. Figure 2(b) presents all the identification results of the phase structures of the ceramics.

In order to study the effects of BKLHZ content on the ferroelectric-paraelectric phase transition of the (1–*x*)KNNS-*x*BKLHZ ceramics, the dielectric-temperature measurements were as well conducted in the temperature range form room temperature to 450 °C, as shown in figure 4. It can be seen that as the temperature rises, the relative dielectric constant ε_r of all the compositions experience a trend of increasing first and then decreasing, accompanying with the appearance of an obvious dielectric peak, which is related to the ferroelectric-paraelectric phase transition. The temperature of the dielectric peak can be approximately determined as the Curie temperature T_C (also known as the Curie point), and one can note that the T_C undergoes a gradual declination with the addition of BKLHZ. In addition, it is found that the dielectric peak has a sharp shape for compositions $x \leqslant 0.035$, indicating that they should be normal ferroelectrics. Nevertheless, the peak tends to broaden with the further increase of BKLHZ content, showing the characteristics of diffusion phase transition. The broadening phenomena in the Curie peak is generally related to the atomic and field disorders, as pointed out by Shvartsman *et al* [35]. In this study, it is the added BKLHZ, which consists of many cations different from those of KNNS, that leads to these disorders.

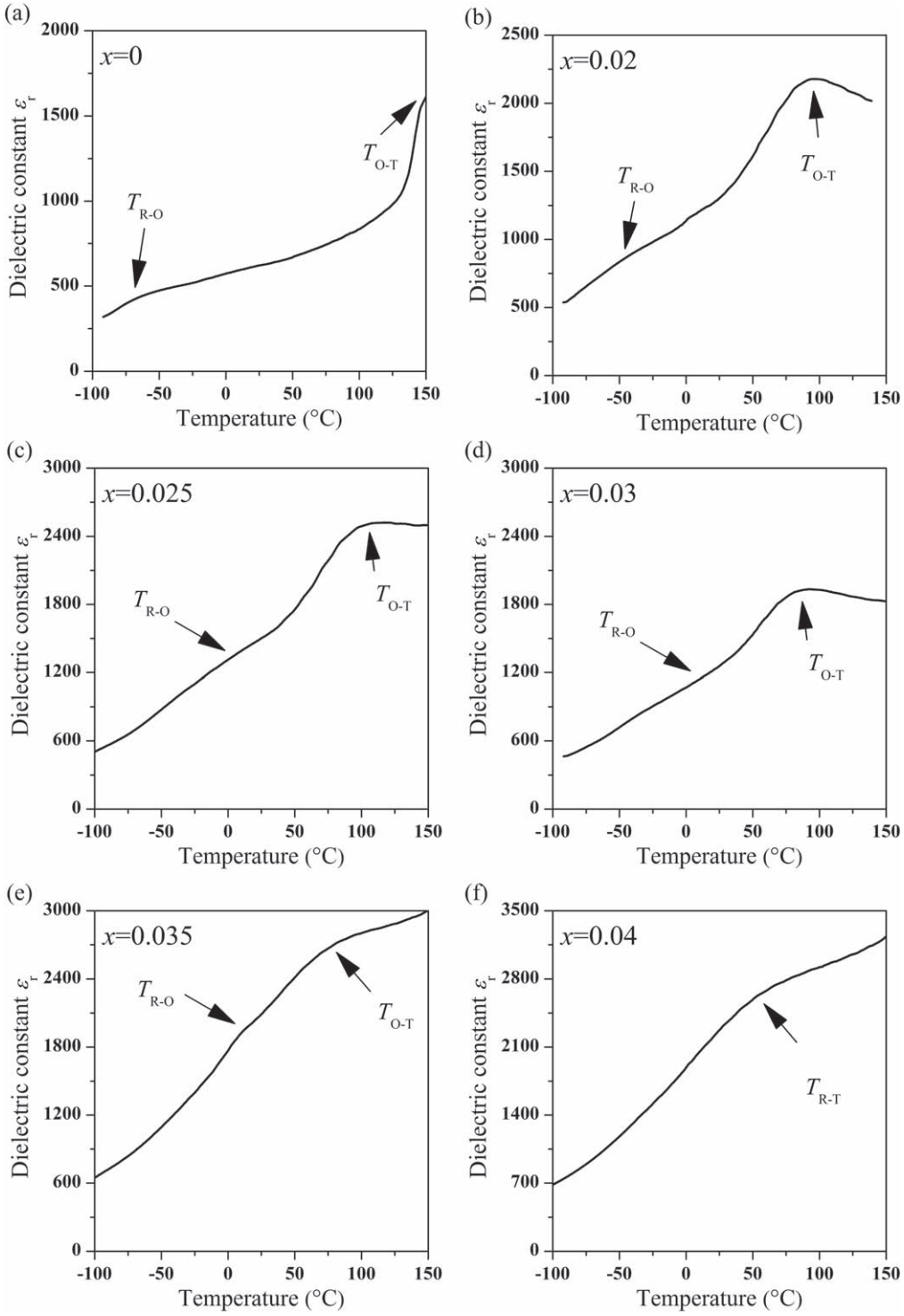

Figure 3. Dielectric-temperature curves of the $(1-x)$KNNS-xBKLHZ ceramics in the temperature range from −100 to 150 °C, measured at 100 kHz, with (a) $x = 0$; (b) $x = 0.02$; (c) $x = 0.025$; (d) $x = 0.03$; (e) $x = 0.035$; (f) $x = 0.04$.

A rough phase diagram is established for the $(1–x)$KNNS-xBKLHZ system in figure 5, whose critical temperatures are obtained from figures 3 and 4. It is noted that the orthorhombic phase region, which lies between the R–O and O–T phase boundaries, tends to shrink with increasing BKLHZ content until at $x = 0.03$, where the R–O and O–T phase boundaries are so close to each other that a three-phase region of R–O–T phases can be considered to be formed in here, just as discussed in previous paragraphs. With the further increase of BKLHZ content, a two-phase region of R–T phases (i.e., the R–T phase boundary) is observed to locate between the rhombohedral and tetragonal single-phase regions.

Figure 6 illustrates the composition-dependent electrical properties of the poled $(1-x)$KNNS-xBKLHZ ceramics, measured at room temperature. It can be seen that both the d_{33}

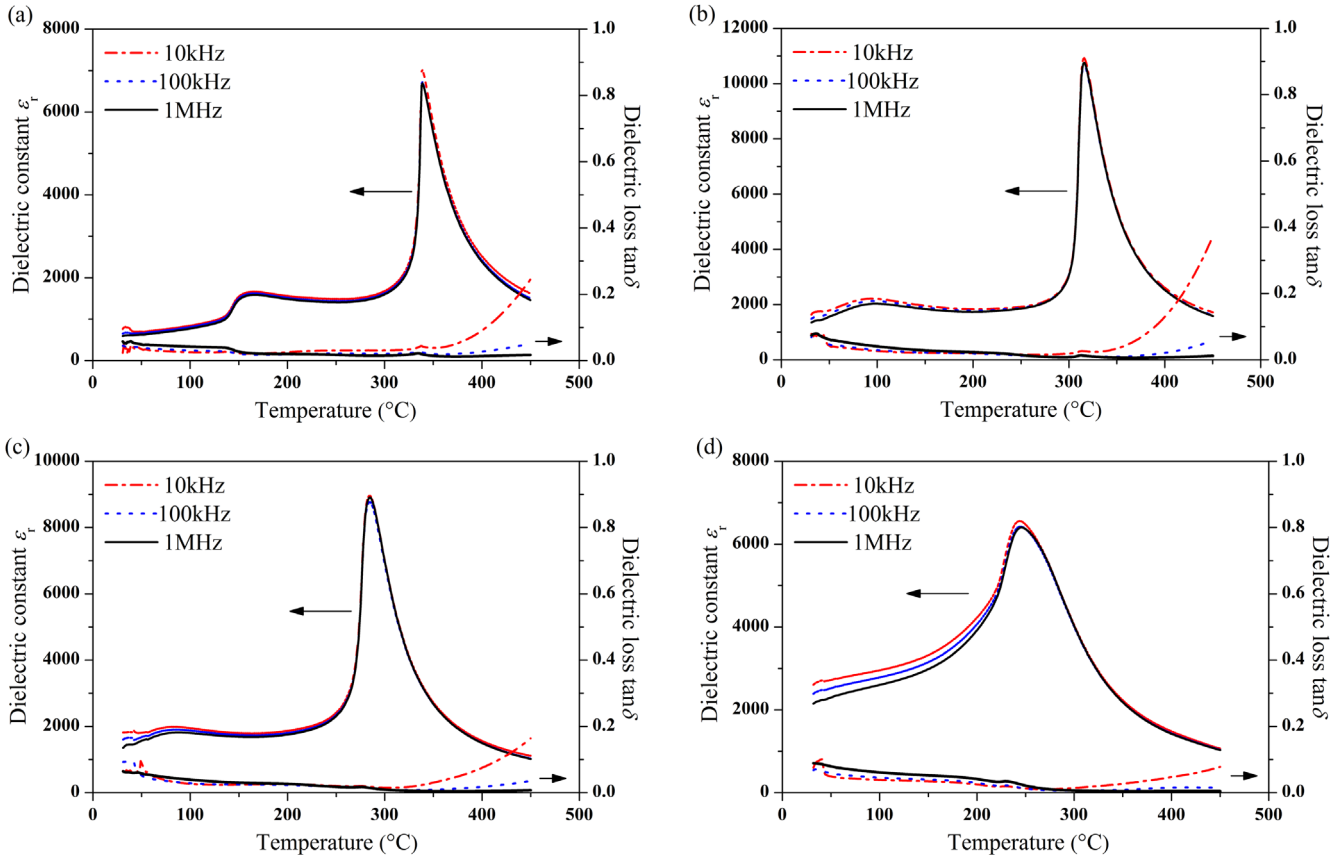

Figure 4. Temperature dependence of the dielectric constant and loss for the $(1-x)$KNNS-xBKLHZ ceramics measured in the temperature range from room temperature to 450 °C: (a) $x = 0$; (b) $x = 0.02$; (c) $x = 0.035$; (d) $x = 0.04$.

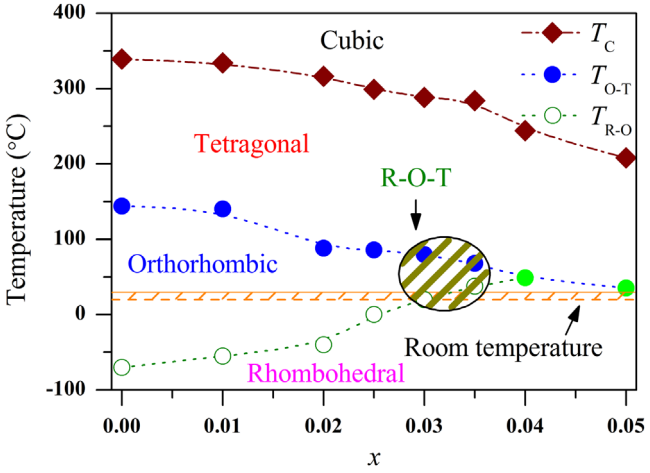

Figure 5. Phase diagram of the $(1-x)$KNNS-xBKLHZ solid solution.

and k_p have a same variation tendency that they firstly increase and then decrease with the addition of BKLHZ, and their maximum values both appear at $x = 0.03$, with $d_{33} = 253$ pC/N and $k_p = 0.36$. Obviously, it is the three-phase coexistence of R–O–T phases that contributes to the enhanced piezoelectric properties. There are two usual explanations on the origin of the enhancing effect for the piezoelectric ceramics with compositions near a phase boundary: (i) the existence of more spontaneous polarization directions facilitate the switching of domains during poling [1, 2]; (ii) the mobility of domain walls can be enhanced in compositions around a phase boundary [36]. Nevertheless, the relative dielectric constant ε_r, which were measured at 10 kHz, remains an almost gradual increasing trend with x within the studied composition range. Hollenstein *et al* [37] found that an appropriate addition of Li^+ ions into the KNN-based ceramics could increase the dielectric constant at near room temperature. Therefore, we believe that it also might be the added Li^+ ions, which are contained in the end-member compound BKLHZ, that lead to the continuous growing in the ε_r in this work.

Thermal stability is one of the key factors for practical application of piezoelectric materials. In the present work, the thermal-depoling behavior of the piezoelectric constant d_{33} was investigated for the $(1-x)$KNNS-xBKLHZ ceramics with compositions near the R–O–T phase coexistence region, as shown in figure 7. The d_{33} was measured at room temperature after the poled ceramic samples were annealed at each annealing temperature (T_A) for 30 min. One can note that the d_{33} gradually decreases with the increase of T_A, and as the T_A closes to the T_C, it then experiences a sharp reduction until complete depolarization is achieved, just as observed in other KNN-based ceramics [18].

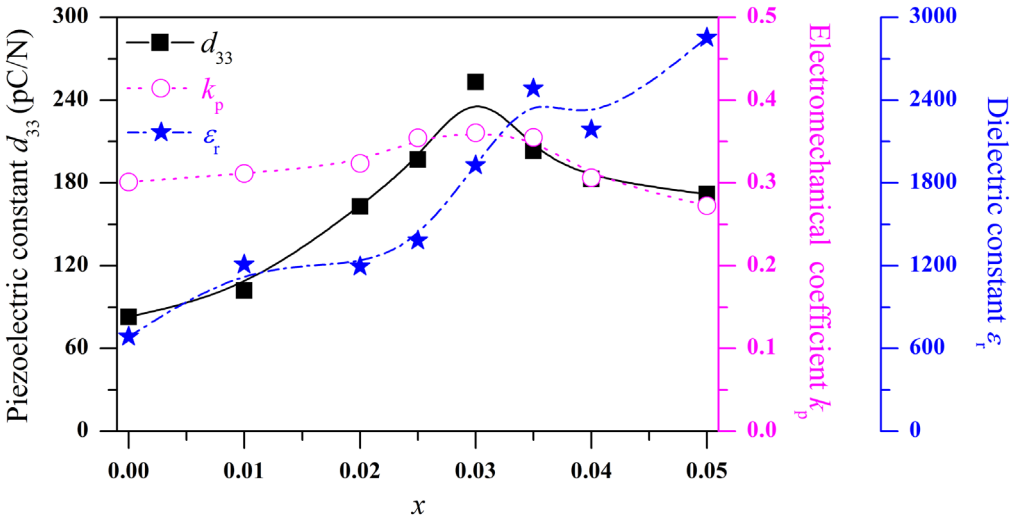

Figure 6. Room-temperature dielectric and piezoelectric properties of the (1−*x*)KNNS-*x*BKLHZ ceramics.

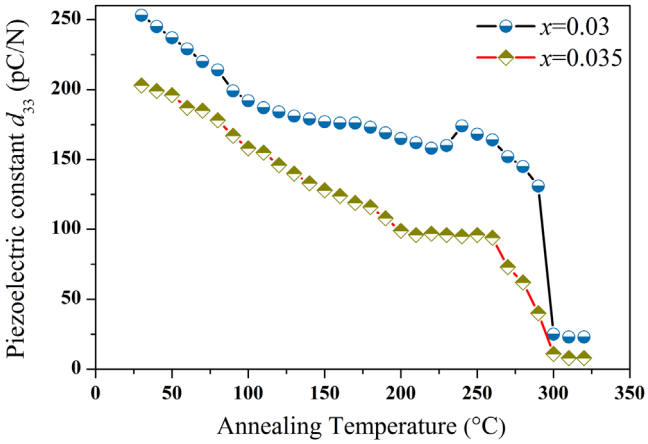

Figure 7. Thermal stability of d_{33} for the (1-*x*)KNNS-*x*BKLHZ ceramics with $x = 0.03$ and 0.035.

4. Conclusion

The new lead-free piezoelectric ceramic system of (1−*x*) KNNS-*x*BKLHZ were prepared by a traditional solid-state sintering method. All the ceramics possess a pure perovskite structure, and their phase structure transition from a single orthorhombic structure to a coexistence of multiple phases with the addition of BKLHZ. Three types of phase boundaries, including the R–O, R–O–T, R–T phase boundaries, are found to be respectively formed in different composition ranges of the ceramic system. The ceramics exhibit enhanced piezoelectric properties for compositions near the R–O–T phase boundary, with the largest piezoelectric constant d_{33} of 253 pC/N and the highest planar electromechanical coupling coefficient of 0.36. These experiment results can provide a useful reference for the development of KNN-based lead-free piezoelectric ceramics.

Acknowledgments

This work was supported by the Fundamental Research Funds for the Central Universities (No. SWU117018), Undergraduate Innovation and Entrepreneurship Training Programs of Chongqing Municipality (No. S201910635069) and Southwest University (No. X201910635281), and Research Project of Chongqing Municipal Education Commission (No. yjg183037). The authors are also grateful for the grant support provided by the 'Zeng Sumin Cup' Research Project (No. zsm20190623) of School of Materials and Energy, Southwest University, China.

ORCID iDs

Yi Chen https://orcid.org/0000-0002-3903-5142

References

[1] Wu J 2018 *Advances in Lead-free Piezoelectric Materials* (Singapore: Springer Nature Singapore Pte Ltd)
[2] Jaffe B, Cook W R Jr and Jaffe H 1971 *Piezoelectric Ceramics* (New York: Academic)
[3] Bell A J and Deubzer O 2018 Lead-free piezoelectrics—the environmental and regulatory issues *MRS Bull.* **43** 581–7
[4] Ibn-Mohammed T, Koh S C L, Reaney I M, Acquaye A, Wang D, Taylor S and Genovese A 2016 Integrated hybrid life cycle assessment and supply chain environmental profile evaluations of lead-based (lead zirconate titanate) versus lead-free (potassium sodium niobate) piezoelectric ceramics *Energy Environ. Sci.* **9** 3495–520
[5] Cross E 2004 *Lead-free at last Nature* **432** 24–5
[6] Zheng T, Wu J, Xiao D and Zhu J 2018 Recent development in lead-free perovskite piezoelectric bulk materials *Prog. Mater. Sci.* **98** 552–624
[7] Shibata K, Wang R, Tou T and Koruza J 2018 Applications of lead-free piezoelectric materials *MRS Bull.* **43** 612–6
[8] Rödel J and Li J 2018 Lead-free piezoceramics: status and perspectives *MRS Bull.* **43** 576–80

[9] Rödel J, Webber K G, Dittmer R, Jo W, Kimura M and Damjanovic D 2015 Transferring lead-free piezoelectric ceramics into application *J. Eur. Ceram. Soc.* **35** 1659–81

[10] Li J, Wang K, Zhu F, Cheng L and Yao F 2013 K,Na)NbO_3-based lead-free piezoceramics: fundamental aspects, processing technologies, and remaining challenges *J. Am. Ceram. Soc.* **96** 3677–96

[11] Xu K, Li J, Lv X, Wu J, Zhang X, Xiao D and Zhu J 2016 Superior piezoelectric properties in potassium–sodium niobate lead-free ceramics *Adv. Mater.* **28** 8519–23

[12] Wu B, Wu H, Wu J, Xiao D, Zhu J and Pennycook S J 2016 Giant piezoelectricity and high Curie temperature in nanostructured alkali niobate lead-free piezoceramics through phase coexistence *J. Am. Chem. Soc.* **138** 15459–64

[13] Wang X, Wu J, Xiao D, Zhu J, Cheng X, Zheng T, Zhang B, Lou X and Wang X 2014 Giant piezoelectricity in potassium−sodium niobate lead-free ceramics *J. Am. Chem. Soc.* **136** 2905–10

[14] Zheng T *et al* 2017 The structural origin of enhanced piezoelectric performance and stability in lead free ceramics *Energy Environ. Sci.* **10** 528–37

[15] Liu Y, Ding Y, Du X, Shi M, He C, Li J, Dai X, Xu Z and Chen Y 2019 Evolution of phase structure, microstructure and piezoelectric properties in $(1-x)(K_{0.4}Na_{0.6})Nb_{0.96}Sb_{0.04}O_3$–$xCa_{0.1}(Bi_{0.5}K_{0.5})_{0.9}ZrO_3$ lead-free ceramics *J. Mater. Sci: Mater. Electron.* **30** 17856–62

[16] Yu Y, Li J, Dai X, Yi Y, Pan Y, He C, Liu Y, Liu X and Chen Y 2019 Composition-driven phase evolution and piezoelectric properties of $(1-x)(K_{0.48}Na_{0.52})_{0.96}Li_{0.04}Nb_{0.95}Sb_{0.05}O_3$-$xBi_{0.5}(Na_{0.84}K_{0.16})_{0.48}Ba_{0.02}ZrO_3$ lead-free ceramics *Mater. Res. Express* **6** 106322

[17] Liu Y, Yi Y, Yu Y, Pan Y, He C, Liu X, Xu Z, Liu G and Chen Y 2019 Microstructures, phase evolution and electrical properties of $(1-x)K_{0.40}Na_{0.60}Nb_{0.96}Sb_{0.04}O_3$-$xBi_{0.5}K_{0.5}HfO_3$ lead-free ceramics *Ceram. Int.* **45** 6328–34

[18] Pan Y, Yu Y, Yi Y, Liu Y, Li J, Dai X, He C, Liu X and Chen Y 2019 Structural evolution and electrical properties of lead-free $(1-x)(K_{0.4}Na_{0.6})Nb_{0.96}Sb_{0.04}O_3$-$xBa_{0.1}(Bi_{0.5}Na_{0.5})_{0.9}ZrO_3$ ceramics *Physica B* **558** 122–6

[19] Chen Y, Liu Y, Xue D, Xu Z, Liu G, Liu X, Chen Z and Jiang X 2018 Effects of $BaHfO_3$ addition on the phase transition and piezoelectric properties of (K,Na)NbO_3-based ceramics *J. Alloy. Compd.* **735** 68–74

[20] Saito Y, Takao H, Tani T, Nonoyama T, Takatori K, Homma T, Nagaya T and Nakamura M 2004 Lead-free piezoceramics *Nature* **432** 84–7

[21] Wang K, Malič B and Wu J 2018 Shifting the phase boundary: potassium sodium niobate derivates *MRS Bull.* **43** 607–11

[22] Xing J, Zheng T, Wu J, Xiao D and Zhu J 2018 Progress on the doping and phase boundary design of potassium–sodium niobate lead-free ceramics *J. Adv. Dielect.* **8** 1830003

[23] Wu J, Xiao D and Zhu J 2015 Potassium−sodium niobate lead-free piezoelectric materials: past, present, and future of phase boundaries *Chem. Rev.* **115** 2559–95

[24] Guo Y, Kakimoto K and Ohsato H 2004 Phase transitional behavior and piezoelectric properties of $(Na_{0.5}K_{0.5})NbO_3$–$LiNbO_3$ ceramics *Appl. Phys. Lett.* **85** 4121–3

[25] Chen Y, Xue D, Ma Y, Chen Z, Jiang X, Liu G and Liu X 2016 Piezoelectric and dielectric properties of $0.995K_{0.48}Na_{0.48}Li_{0.04}Nb_{(1-x)}Sb_xO_3$–$0.005BiAlO_3$ lead-free piezoelectric ceramics *Mater. Res. Bull.* **84** 240–4

[26] Guo Y, Kakimoto K and Ohsato H 2005 $Na_{0.5}K_{0.5})NbO_3$–$LiTaO_3$ lead-free piezoelectric ceramics *Mater. Lett.* **59** 241–4

[27] Liu C, Xiao D, Huang T, Wu J, Li F, Wu B and Zhu J 2014 Composition induced rhombohedral–tetragonal phase boundary in $BaZrO_3$ modified $(K_{0.445}Na_{0.50}Li_{0.055})NbO_3$ lead-free ceramics *Mater. Lett.* **120** 275–8

[28] Yang Y, Dai Q, Chen T, Liu Y, Zhang T and Zhang J 2019 Role of $BiScO_3$ in phase structure and electrical properties of potassium sodium niobate ternary materials *J. Alloy. Compd.* **770** 466–72

[29] Xiang R and Wu J 2016 Contribution of $Bi_{0.5}Na_{0.5}ZrO_3$ on phase boundary and piezoelectricity in $K_{0.48}Na_{0.52}Nb_{0.96}Sb_{0.04}O_3$-$Bi_{0.5}Na_{0.5}SnO_3$-$xBi_{0.5}Na_{0.5}ZrO_3$ ternary ceramics *J. Alloy. Compd.* **684** 397–402

[30] Li P, Huan Y, Yang W, Zhu F, Li X, Zhang X, Shen B and Zhai J 2019 High-performance potassium-sodium niobate lead-free piezoelectric ceramics based on polymorphic phase boundary and crystallographic texture *Acta Mater.* **165** 486–95

[31] Lv X, Li Z, Wu J, Xi J, Gong M, Xiao D and Zhu J 2016 Enhanced piezoelectric properties in potassium-sodium niobate-based ternary ceramics *Mater. Des.* **109** 609–14

[32] Hu Q, Du H, Feng W, Chen C and Huang Y 2015 Studying the roles of Cu and Sb in $K_{0.48}Na_{0.52}NbO_3$ lead-free piezoelectric ceramics *J. Alloy. Compd.* **640** 327–34

[33] Zhang B, Wang X, Cheng X, Zhu J, Xiao D and Wu J 2013 Enhanced d_{33} value in $(1-x)[(K_{0.50}Na_{0.50})_{0.97}Li_{0.03}Nb_{0.97}Sb_{0.03}O_3]$-$xBaZrO_3$ lead-free ceramics with an orthorhombic–rhombohedral phase boundary *J. Alloys Compd.* **581** 446–51

[34] Cai K, Yan X, Deng P, Jin L, Bai Y, Zeng F and Guo D 2019 Phase coexistence and evolution in sol-gel derived BY-PT-PZ ceramics with significantly enhanced piezoelectricity and high temperature stability *J. Materiomics* **5** 394–403

[35] Shvartsman V V and Lupascu D C 2012 Lead-free relaxor ferroelectrics *J. Am. Ceram. Soc.* **95** 1–26

[36] Damjanovic D 2005 Contributions to the piezoelectric effect in ferroelectric single crystals and ceramics *J. Am. Ceram. Soc.* **88** 2663–76

[37] Hollenstein E, Damjanovic D and Setter N 2007 Temperature stability of the piezoelectric properties of Li-modified KNN ceramics *J. Eur. Ceram. Soc.* **27** 4093–7